

Experimental investigation of flux motion in exponentially shaped Josephson junctions

G. Carapella,* N. Martucciello, and G. Costabile

*Departement of Physics “E. R. Caianiello”,
and INFM Research Unit, University of Salerno,
via S. Allende, I-84081 Baronissi, Italy.*

(Dated: November 3, 2018)

Abstract

We report experimental and numerical analysis of exponentially shaped long Josephson junctions with lateral current injection. Quasi-linear flux flow branches are observed in the current-voltage characteristic of the junctions in the absence of magnetic field. A strongly asymmetric response to an applied magnetic field is also exhibited by the junctions. Experimental data are found in agreement with numerical predictions and demonstrate the existence of a geometry-induced potential experienced by the flux quanta in nonuniform width junctions.

PACS numbers: 74.50.+r

I. INTRODUCTION

In recent years, there have been some theoretical studies concerning the possibility to influence the flux motion in long Josephson junctions by mean of geometry-induced or field-induced potentials. The most known example is the annular junction embedded in a spatially homogeneous magnetic field. As it is known¹, in this case a cosinusoidal potential is experienced by a flux quantum trapped in the junction when a spatially homogeneous magnetic field is applied parallel to the junction barrier. The origin of the potential is caused by the spatial variation of the radial component of the magnetic field that in this special geometry becomes sinusoidal. A field-induced sawtooth-like potential has been recently considered² for experimental demonstration³ of ratchet effect in annular junctions. Currently, modifications of the annular geometry, as the heart-shaped geometry⁴ are used to achieve a field-induced double-well potential for demonstration of fluxon quantum-bit and macroscopic quantum coherence phenomena.

To achieve potentials without the help of a magnetic field, the case of a nonuniform junction width has been theoretically addressed in recent years for linear^{5,6,7,8} as well as for annular⁹ geometries. Theoretically, a geometry-induced potential related to the spatial variation of the junction width is expected. This potential corresponds to a force acting on the fluxons in the direction of the shrinking width. Recently,¹⁰ ordinary Josephson flux-flow oscillators^{11,12} have been modified adding to the classical overlap geometry¹³ unbiased pointed tails. This is expected to enhance the annihilation of the fluxons at the edges of the oscillator, with consequent reduction of fine structures in the ordinary velocity-matching step^{11,12,14}.

In this paper we experimentally address the existence of the geometrical force in nonuniform width junctions. To do this, we consider an exponentially shaped overlap junction with lateral current injection. The lateral current injection acts as a flux quanta generator, also in the absence of a magnetic field, while the unbiased shaped region should act as an accelerating region for both fluxons or antfluxons injected at one edge of the junction. If really present, the geometric force should allow to achieve a quite regular unidirectional flux flow motion in the junction, without the help of a magnetic field. This dynamical regime should be accounted for a branch in the current-voltage curve of the shaped junction. The demonstration of such branches in the current-voltage curves of shaped junctions we fabricated

suggests that such a geometrical force is really experienced by the flux quanta.

The paper is organized as follows. In Sec. II we specialize the general model^{6,7} for a long junction with nonuniform width to our exponentially shaped junction with lateral current injection. In Sec. III the experimental results both in the absence of magnetic field and in the presence of magnetic field are presented and discussed with the help of numerical simulations. Finally, main results are summarized in the Conclusions.

II. THEORY

Under some simplifcative hypotheses⁶, the model for a long overlap junction with nonuniform width $W(x) = f_1(x) - f_2(x)$ was found as^{6,7}

$$\phi_{xx} - \phi_{tt} = \sin \phi + \alpha \phi_t - \frac{W'(x)}{W(x)} \phi_x + \eta_y \frac{W'(x)}{W(x)} - \Gamma(x), \quad (1)$$

with

$$\Gamma(x) = \frac{\eta_x|_{f_2} - \eta_x|_{f_1}}{W(x)}. \quad (2)$$

In Eq. (1) ϕ is the Josephson phase, α is the dissipation parameter, η_x and η_y are the normalized magnetic fields in the x and y directions, respectively. Space is normalized to the Josephson penetration length λ_J and time to the inverse of the plasma frequency $\omega_J = \bar{c}/\lambda_J$, with \bar{c} the velocity of electromagnetic waves in the junction. For the geometry we report here (see Fig. 1) the total physical length of the junction is $L = L_0 + L_S + L_L \gg \lambda_J$, while the width is chosen as

$$W(x) = \begin{cases} W_0 & 0 < x \leq L_0, \\ W_0 \exp \left[\frac{1}{L_S} \ln \left(\frac{W_L}{W_0} \right) (x - L_0) \right] & L_0 < x \leq L_S + L_0, \\ W_L & L_S + L_0 < x \leq L, \end{cases} \quad (3)$$

The bias current I can be fed into the left or into the right edge, as shown in Fig. 1. The bias term $\Gamma(x)$ in Eq. (2) becomes

$$\gamma_A(x) = \begin{cases} \frac{IL}{J_0 L_0 W_0 L} \equiv \gamma \frac{L}{L_0} & 0 < x \leq L_0, \\ 0 & L_0 < x \leq L, \end{cases} \quad (4)$$

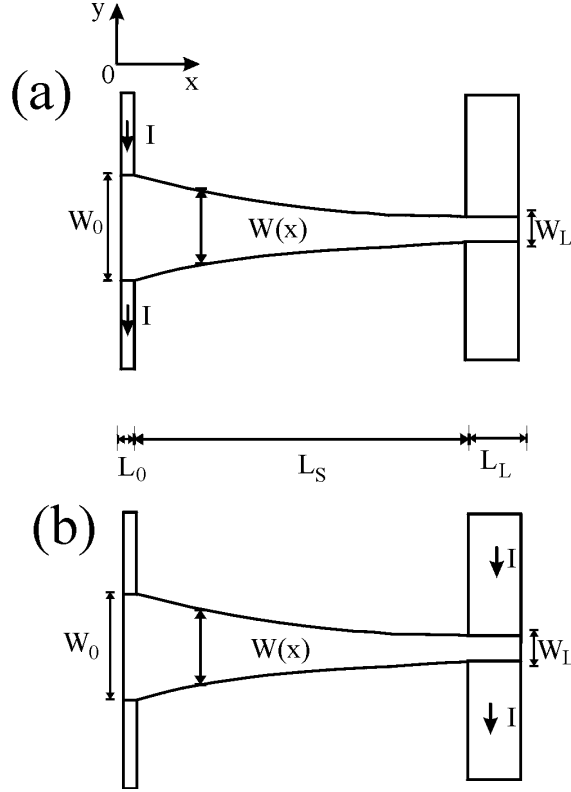


FIG. 1: Exponentially shaped junction with lateral current injection. The current can be fed into the left [(a)] or into the right [(b)] edge.

for left edge current injection, and

$$\gamma_B(x) = \begin{cases} 0 & 0 < x \leq L_S + L_0, \\ \frac{iL}{j_0 L_L W_L L} \equiv \gamma \frac{L}{L_L} & L_S + L_0 < x < L, \end{cases} \quad (5)$$

for right edge current injection. The lengths L_0 , L_L , W_0 , and W_L are chosen to be shorter than λ_J and such that $L_L W_L = L_0 W_0$, to have equal biased areas.

Hence, the model for our exponentially shaped junction becomes

$$\phi_{xx} - \phi_{tt} = \sin \phi + \alpha \phi_t + \lambda \phi_x - \eta \lambda - \gamma_{A,B}(x), \quad (6a)$$

$$\phi_x(0) = \eta, \quad (6b)$$

$$\phi_x(l) = \eta, \quad (6c)$$

where $l = L/\lambda_J$, $\lambda = \lambda_J \ln(W_0/W_L)/L_S$, and η accounts for an external magnetic field applied in the y direction. We remark that the chosen geometry reduces to the exponentially

shaped in-line geometry^{7,8} in the case of left current injection with injection length L_0 much lower than λ_J . In such a limit, the model becomes

$$\phi_{xx} - \phi_{tt} = \sin \phi + \alpha \phi_t + \lambda \phi_x - \eta \lambda, \quad (7a)$$

$$\varphi_x(0) = \eta - \gamma l, \quad (7b)$$

$$\varphi_x(l) = \eta. \quad (7c)$$

As first noted in Ref. 6, a force that drags fluxons or antfluxons in the direction of the narrowing width is expected for our geometry. In fact, in the absence of magnetic field ($\eta = 0$), for a soliton

$$\phi(x) = 4 \arctan \left[\exp \left[\sigma \frac{x - ut}{\sqrt{1 - u^2}} \right] \right]$$

in the unbiased region [$\gamma_{A,B}(x) = 0$], the following equation of motion can be found from Eqs. (6) in the framework of the perturbative approach¹⁵

$$(1 - u^2)^{-3/2} \frac{du}{dt} = -\alpha \frac{u}{\sqrt{1 - u^2}} + \frac{\lambda}{\sqrt{1 - u^2}}. \quad (8)$$

This indicates that, if present, both a fluxon or an antfluxon will experience a force proportional to the shaping parameter λ and will be accelerated in the narrowing width direction, i.e. from the left to the right in our geometry. From Eq. (8) the stationary velocity of the motion will be $u = \lambda/\alpha$ for $\lambda/\alpha < 1$ or the limit velocity $u = 1$ for $\lambda/\alpha > 1$.

III. NUMERICAL AND EXPERIMENTAL RESULTS

We realized Nb/Al₂O₃/Nb junctions with the geometry shown in Fig. 1. The physical dimensions of the junctions were $L = L_0 + L_s + L_L = (10 + 560 + 40) \mu\text{m}$, $W_0 = 40 \mu\text{m}$, $W_L = 10 \mu\text{m}$. For the two junctions we report here the normalized lengths were $l \approx 20$, and $l \approx 17$, with shaping parameters $\lambda \approx 0.07$ and $\lambda \approx 0.08$, respectively. In the following the behavior of the junctions in the absence of magnetic field as well as the response to a magnetic field applied along the y direction is discussed.

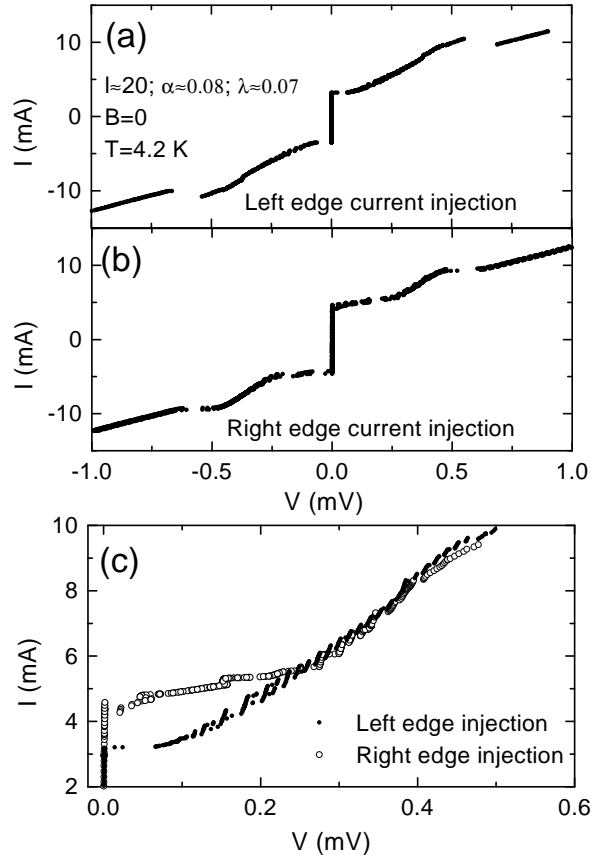


FIG. 2: Current-voltage curve of a junction with left current injection (a) or with right current injection (b) exhibiting quasi-linear flux flow branches. In (c) the flux flow branch for left current injection is compared with the one achieved for right current injection.

A. Behavior in the absence of magnetic field

The current-voltage curve for the junction with $l \approx 20$ is reported in Fig. 2. No external magnetic field is applied to the junction. Panel (a) of this figure refers to the case of current injected into the left edge, while the panel (b) refers to the case of current injected into the right edge. In both cases an almost linear branch starting from a certain critical current and extending for a given current range is observed, but some qualitative differences exist between the two cases. As better seen in Fig. 2(c), when current is injected into the left edge the branch starts to a lower critical current and is more regular than the branch achieved with current injected to the right edge. The observed behavior seems to be consistent with the idea that a geometrical force is effectively experienced by the fluxons in this geometry. When

current of positive (negative) polarity is injected into the left edge, antfluxons (fluxons) will enucleate at this edge after a critical current value has been reached. From Eq. (8) these antfluxons are expected to be accelerated toward the other edge because of the geometrical force, so realizing a regular unidirectional flux motion. Conversely, if the current is injected into the right edge, the antfluxons enucleated at this edge should overcome a force to travel toward the left edge. This should result in an irregular or chaotic flux motion. Moreover, in the left current injection the geometrical force helps to start an antfluxon (or fluxon) motion, corresponding to a voltage in the I-V curve beyond a critical current value. In the right current injection such a force opposes the starting of the flux motion, so resulting in a larger critical current.

We should remark that the quasi-linear branches reported in Fig. 2 could remind the Displaced Linear Slope branches sometimes reported for rectangular in-line or overlap geometries^{16,17,18,19,20}. However here the branches are rather regular, quite noiseless, and are obtained in the absence of magnetic field.

In the following we will focus on the left current injection. In Fig. 3(a) same data of Fig. 2(a) are replotted on a larger scale. As better seen in the inset, the flux flow branch exhibits a series of small steps spaced of a voltage $\Delta V \approx 15 \mu\text{V}$. The curve reminds the numerically predicted curve for an exponential shaped asymmetric in-line junction⁸. The observed voltage spacing is consistent with the spacing of cavity mode resonances expected from physical dimensions of our junction, $\Delta V \simeq \Phi_0 \bar{c}/L$. This is to be expected due to the open boundary condition at the edges. The antfluxons in the chain moving toward the right edge will be reflected as fluxons. If the dissipation α is not too large, the antfluxons can have enough energy to travel toward the left edge as fluxons after the reflection, despite of the geometrical force opposing the motion. This mechanism can excite cavity mode resonances. However, for quite large dissipation one expect that the reflected motion would be more and more damped, and the excitation of cavity modes should be consequently damped. In Fig. 3(b) the I-V curve of the junction with $l \approx 17$ is plotted for three different temperatures, corresponding to three different α values. As expected, the small steps accounting for the cavity mode resonances are more and more damped as the dissipation (temperature) is increased.

To gain further insight in the flux motion dynamics in the absence of magnetic field, we integrated the model Eqs. (6) with $\eta = 0$ and forcing term $\gamma_A(x)$ defined in Eq. (4). In

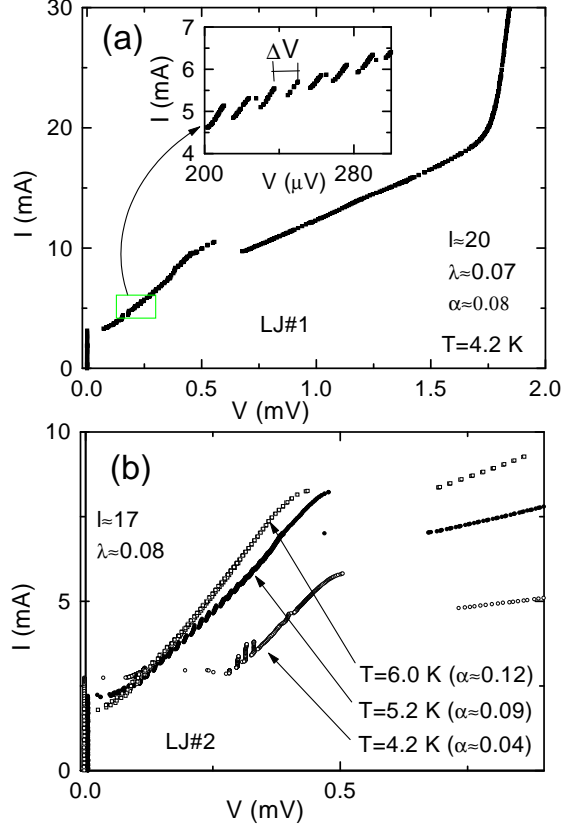


FIG. 3: (a) The current-voltage curve of Fig. 2(a) is replotted on a larger scale. Small steps in the flux-flow branch are shown in the inset. (b) Flux flow branch of a junction with $\lambda \approx 0.08$ at different temperatures.

Fig. 4(a) we show the calculated current voltage curve for a junction with left edge current injection and of uniform width [$\lambda = 0$ in Eqs. (6)]. This is equivalent to the asymmetric in-line rectangular geometry¹³. As seen in the snapshot showing the instantaneous voltage distribution in the junction, antfluxons are created at the biased edge. However, due to the absence of a force in the unbiased region, the flux motion is not very regular. Here it is only the repulsion between flux quanta that tends to drive the flux toward the right edge. The resulting motion is quite noisy, as well as the calculated ac voltage at the right edge.

In Fig. 4(b) the case of an exponentially shaped width ($\lambda = 0.07$) is considered. In the simulation we used parameters similar to the ones estimated for the experimental curve in Fig. 3(b). As it seen in the snapshot, now the presence of a force in the unbiased region makes the flux motion toward the right edge more regular, as well as the voltage signal at the right edge. In the snapshot four moving antfluxon are counted as present in the mean

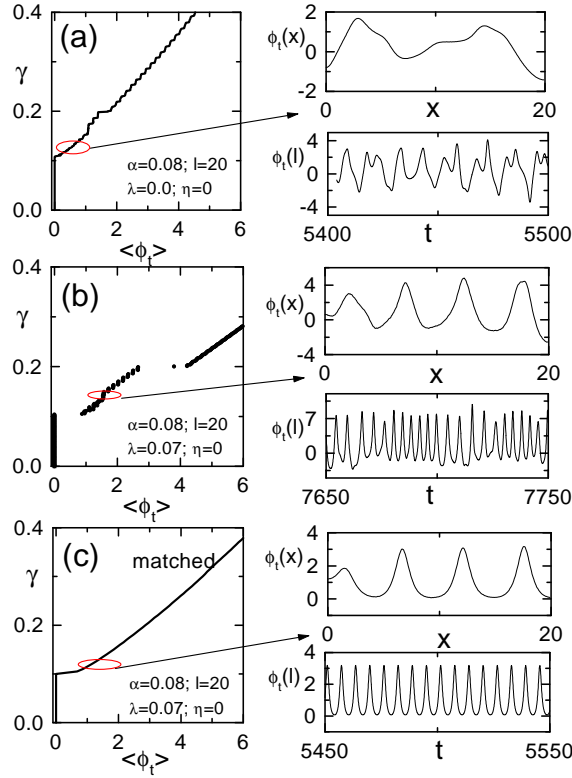


FIG. 4: Calculated current-voltage curve for an unmatched rectangular [(a)], for an unmatched exponentially shaped [(b)], and for a matched exponentially shaped [(c)] junction with lateral current injection. The snapshots shows the instantaneous voltage profiles and the voltage signal at the right edge of the junctions.

in the junction for the chosen bias point. By increasing the bias current, more and more antifluxons can be injected in the junction, and the chain becomes more and more dense. Correspondingly, the voltage signal at the right edge becomes less impulsive and approaches a sinusoidal form. When the junction is completely filled with antifluxons, a transition to a new dynamical regime, similar to a laminar phase flow⁸ is achieved. In the current-voltage curve, this transition corresponds to the switch from the flux flow branch toward the other resistive branch, beyond a critical current value. As in the experimental curve, the small steps in the calculated flux flow branch are spaced of π/l , the spacing (in normalized units) expected from cavity mode resonances excited from reflecting boundary conditions at the edges.

As said above, the resonances can be damped by increasing the dissipation α . However,

another mean to achieve this is to match the impedance of the fluxon chain with a load z at the right edge. The matching is found possible^{7,8} for this geometry, conversely to the rectangular asymmetric in-line geometry. For our exponentially shaped junction the wave impedance is just the stationary velocity we have found above, $-\phi_t/\phi_x = u = \lambda/\alpha$. This should be matched with a load of impedance $z = -\phi_t(l)/\phi_x(l)$. Numerical results for the case of a matched load are shown in Fig. 4(c). As a result of the absence of reflections, the small steps typical of the unmatched case of Fig. 4(b) are now absent and the flux chain exhibits a very regular motion, as well as the voltage signal at the matched edge. This characteristic makes the exponentially shaped junction interesting as zero-magnetic field flux flow oscillator.

In Fig. 5 there are shown numerical results for a junction with $\lambda/\alpha > 1$. For the unmatched case shown in Fig. 5(a) the used parameters can account for the current-voltage curve at $T=4.2$ K in Fig. 3(b). In both cases $\lambda/\alpha > 1$. As said above, in such a case the antfluxons are accelerated toward the asymptotic velocity $u = 1$, so the matching condition is now $z = 1$. In the snapshots shown in Fig. 5(a) and (b) we show also the instantaneous magnetic field. Antifluxons in the chain are accelerated and, due to their relativistic nature, they are Lorentz-contracted as the asymptotic velocity is approached. As for the case $\lambda/\alpha < 1$, the matched junction exhibits a smooth flux-flow branch and the voltage signal at the right edge is very regular.

B. Behavior in the presence of magnetic field

Due to the lateral current injection and due to the existence of a preferred direction of motion, our exponentially shaped junction is expected to show a behavior in magnetic field even more strongly asymmetric with respect to the asymmetric rectangular in-line geometry. The calculated critical current as a function of the magnetic field is shown in Fig. 6(a) for a junction with $l = 20$ and $\lambda = 0.07$. The pattern was obtained integrating Eqs. (6) with $\eta \neq 0$. A quite abrupt decrease of the critical current around $\eta = 2$ is recovered. In normalized units, for this value of magnetic field a fluxon is enucleated in the junction. The almost complete absence of secondary lobes in the pattern means the almost complete absence of trapped flux in this kind of junction, an indication that the geometrical force helps to move fluxons just after their enucleation.

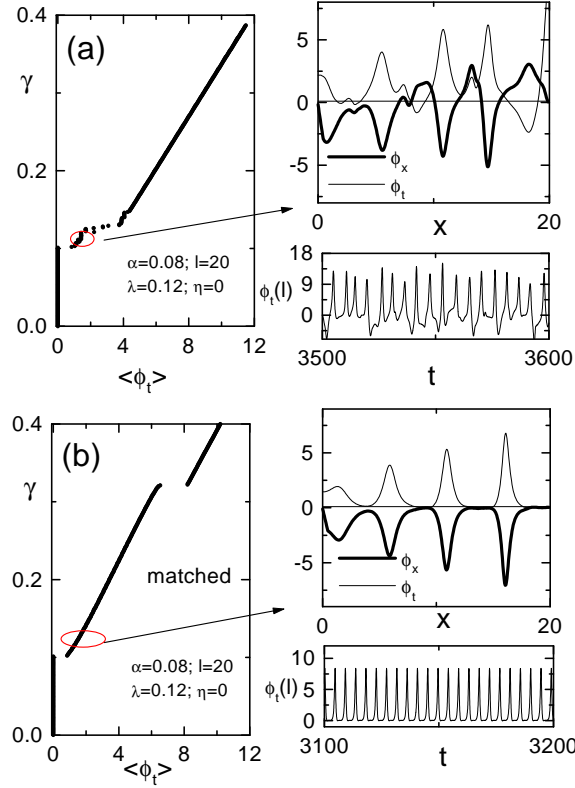


FIG. 5: Calculated current-voltage curve for an unmatched [(a)] and a matched [(b)] exponentially shaped junction with $\lambda = 0.12$. The snapshots shows the instantaneous voltage and magnetic field profiles, and the voltage signal at the right edge of the junctions.

Figure 6(b) shows a global representation of calculated resonant steps achieved for normalized magnetic field values slightly larger than the critical value $\eta = 2$. Such a plot is obtained superimposing the curves corresponding to different values of magnetic field. Two families of steps with two characteristic voltage spacing are recovered. The lower voltage spacing is the one expected for Fiske mode resonances, $\Delta \sim \pi/l$, the larger one is about $2\pi/l = 2\Delta$. The family of steps with larger voltage spacing appears in the same current range where the flux flow branch is achieved in the absence of magnetic field. From numerical simulation it is seen that these steps with larger voltage spacing consists of cavity mode resonances excited by a fluxon chain and an antfluxon chain moving in opposite directions. In fact, for positive bias current an antfluxon chain moving toward the right edge is generated, while a positive magnetic field generate fluxons. These fluxons are pulled toward the left edge by the Lorentz force associated to the positive bias current at this edge. Antifluxons

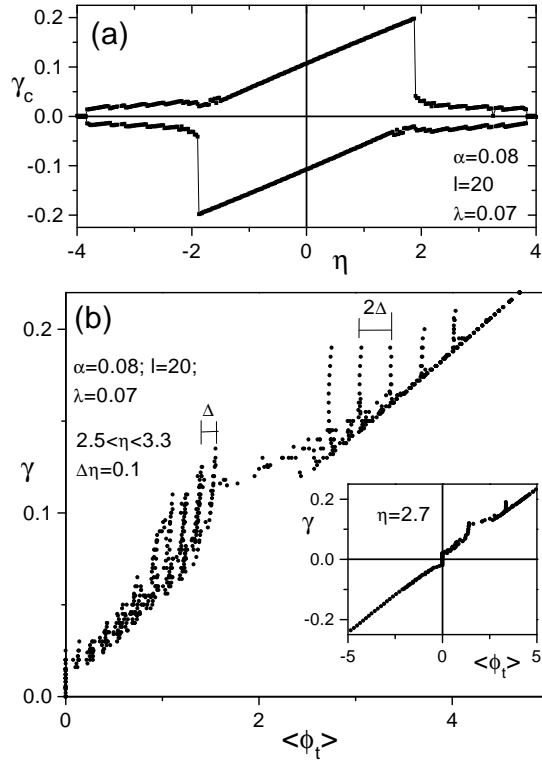


FIG. 6: (a) Calculated magnetic field pattern for a junction with $\lambda = 0.07$. (b) Calculated steps induced in the current voltage characteristic by a magnetic field varied in the range $2.5 < \eta < 3.3$. In the inset the steps at for a given field value are shown.

travelling toward the right generate a voltage with positive polarity that adds to the voltage of the fluxons traveling toward left. This accounts for the larger voltage spacing observed for the steps of this family.

For negative bias currents, the fluxons generated by the positive magnetic field are pushed toward the right edge by the Lorentz force associated to the negative bias current. Moreover, also the fluxon chain injected at the left edge by the bias current moves toward the right, under the action of the geometrical force. The result is that an unidirectional motion toward the right edge tends to be achieved, with consequent damping of resonant steps accounting for cavity mode resonances. As seen in the inset of Fig. 6(b), resonant steps are in fact virtually absent for negative current values. This peculiarity is observed also for larger magnetic values. For negative magnetic fields values, the current-voltage curve show steps for negative bias current values, and no steps for positive bias values. In other words, the current-voltage curve reflects with respect to the origin when the sign of the magnetic field

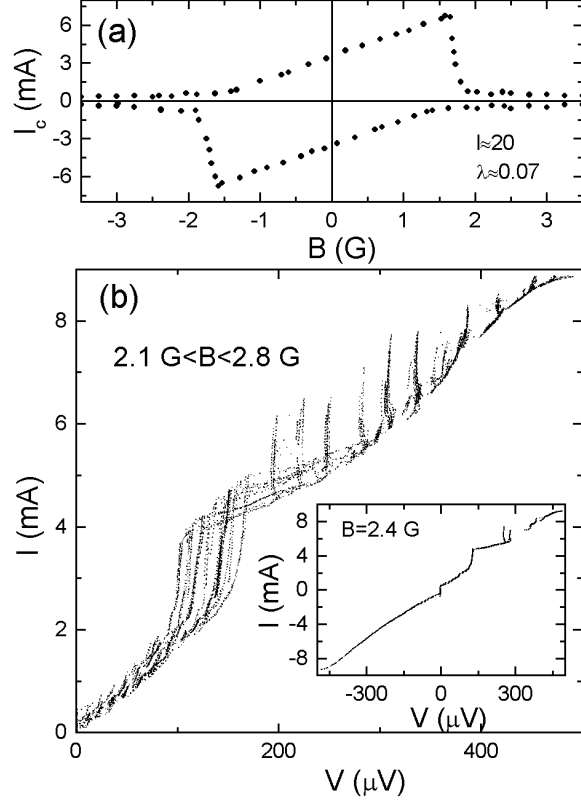


FIG. 7: Measured magnetic field pattern (a) and current steps (b) induced in a junction with $\lambda \approx 0.07$ by a magnetic field slightly larger than the critical field. In the inset the current voltage curve at $B=2.4$ G is shown.

is inverted.

Predicted strongly asymmetric magnetic field behavior summarized in Fig. 6 is fully recovered in the experiment, as shown in Fig. 7. Experimental data refer to the junction with $l \approx 20$. In Fig. 7(b) the steps are achieved for magnetic field values slightly larger than $B_c = 1.75$ G, the critical field of the junction. In Fig. 8(a) we reported the modification of the flux flow branch induced by a low magnetic field, i.e., lower than B_c . An asymmetric tuning of the branch is recovered. This can be easily understood as follows. We are using strongly left-edge-peaked current injection. In this case our junction can be also described as a shaped asymmetric in-line junction, i.e., with model Eqs. (7). Looking at the vortex generator term $\phi_x(0) = \eta - \gamma l$, it is easily understood that a positive magnetic field cooperates with a negative bias current to inject fluxons in the junctions, while such a positive magnetic field opposes a positive current injecting antfluxons in to the junction. The result is that,

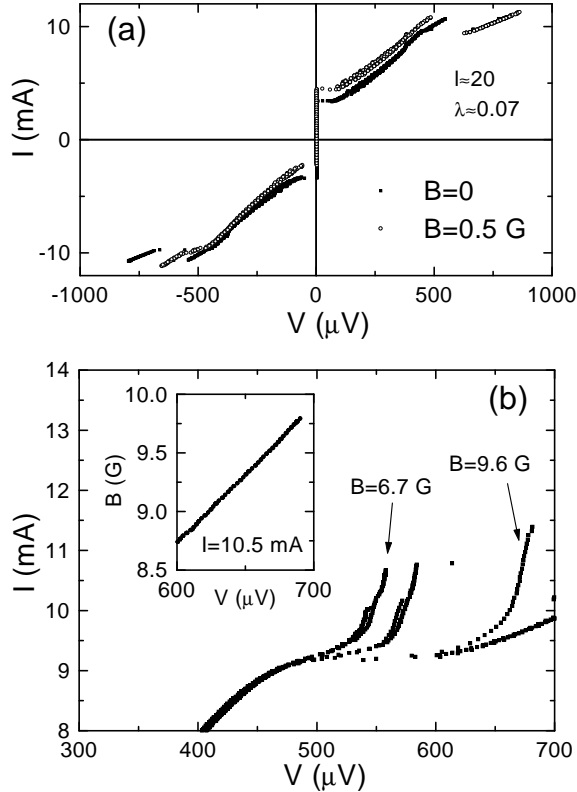


FIG. 8: (a) Modification of the flux flow branch induced by a magnetic field lower than the critical field. (b) Steps recorded for magnetic fields quite larger than the critical field of the junction. A smooth single step is achieved for $B > 8$ G. In the inset we show the voltage of the junction polarized at fixed current on the step as a function of the magnetic field.

for a given absolute value of the bias current, more solitons are present at negative polarities than at positive polarities, resulting in a voltage at negative polarity larger than the voltage at positive polarity, as it is in fact observed in the experimental curves of Fig. 8(a).

Figure 8(b) shows the steps recorded in the junction for magnetic fields quite larger than B_c . The fine structures accounting for Fiske modes are completely smeared out at $B \approx 9$ G and a smooth step, similar to the velocity-matching step^{11,12,14}, with asymptotic voltage strictly proportional to B is achieved. The proportionality between the voltage and the magnetic field is shown in the inset for a given biasing current. The velocity-matching step is found to exist beyond the current-voltage range of existence of the linear flux flow branch in zero field, i.e., beyond $V = 600$ μ V (and up to 1500 μ V) and $I = 9.5$ mA. This is consistent with the observation¹⁴ that the velocity matching step originates from a quasi-linear waves

regime in the junction. In our case such a quasi-linear background is the laminar phase flow⁸ achieved beyond the current range typical of the zero-field flux-flow branch.

IV. CONCLUSIONS

Summarizing, we have experimentally investigated the occurrence of dynamical states in exponentially shaped overlap junctions with lateral current injection. In zero magnetic field, the lateral current injection acts as a fluxon or antifluxon chain generator and these chains can be accelerated by the geometrical force originating from the nonuniform width of the junction. The result is that a quite regular flux-flow motion, corresponding to a quasi-linear branch in the I-V curve of the junction, can be achieved in this kind of junction without the help of an external magnetic field. Moreover, numerical simulations show that this kind of motion can be precisely matched to a load, a peculiarity that makes the zero field flux flow branch interesting for zero-field flux flow oscillators. In the presence of a magnetic field a rather asymmetric behavior is exhibited by the junction. For low magnetic fields an asymmetric tuning of the flux-flow branch is observed, for moderated magnetic field ordinary Fiske modes steps are mixed with nonlinear cavity modes steps, and for quite large magnetic fields a single step similar to the velocity-matching step known for uniform width geometries is recovered.

Acknowledgments

We acknowledge Professor M. Cirillo for providing us with the photolithographic masks we used to fabricate the devices. Fruitful discussions with S. Pagano and C. Nappi, as well as the financial support of MURST COFIN00 are also acknowledged.

* Corresponding author;
e-mail: giocar@sa.infn.it;
FAX: +3908965390

¹ N. Grønbech-Jensen, P. S. Lomdahl, and M. R. Samuelsen, Phys. Rev. B **43**, 12799 (1991).

- ² G. Carapella, Phys. Rev. B **63**, 054515 (2001).
- ³ G. Carapella and G. Costabile, Phys. Rev. Lett. **87**, 077002 (2001).
- ⁴ A. Wallraff, Y. Koval, M. Levitchev, M. V. Fistul, and A. V. Ustinov, J. Low. Temp. Phys. **118**, 543 (2000).
- ⁵ S. Sakai, M. R. Samuelsen, and O. H. Olsen, Phys. Rev. B **36**, 217 (1987).
- ⁶ S. Pagano, C. Nappi, R. Cristiano, E. Esposito, L. Frunzio, L. Parlato, G. Peluso, G. Pepe, and U. Scotti Di Uccio, in *Nonlinear Superconducting Devices and High T_c Materials*, edited by R. D. Parmentier and N. F. Pedersen (World Scientific, Singapore, 1995).
- ⁷ A. Benabdallah, J. G. Caputo, and A. C. Scott, Phys. Rev. B **54**, 16139 (1996).
- ⁸ A. Benabdallah, J. G. Caputo, and A. C. Scott, J. Appl. Phys. **88**, 3527 (2000).
- ⁹ E. Goldobin, A. Sterck, and D. Koelle, Phys. Rev. E **63**, 031111 (2001).
- ¹⁰ V. P. Koshelets, P. N. Dmitriev, A. S. Sobolev, A. L. Pankratov, V. V. Khodos, V. L. Vaks, A. M. Baryshev, P. R. Wesselius, and J. Mygind, to be published in PHYSICA C (2001).
- ¹¹ T. Nagatsuma, K. Enpuku, K. Sueoka, K. Yoshida, and F. Irie, J. Appl. Phys. **58**, 4412 (1985).
- ¹² V. P. Koshelets, S. V. Shitov, A. V. Shuchukin, L. V. Filippenko, J. Mygind, and A. V. Ustinov, Phys. Rev. B **56**, 5572 (1997).
- ¹³ A. Barone and G. Paternó, *Physics and Applications of the Josephson Effect* (John Wiley & Sons, New York, 1982).
- ¹⁴ M. Cirillo, N. Grønbech-Jensen, M. R. Samuelsen, M. Salerno, and G. Verona Rinati, Phys. Rev. B **58**, 12377 (1998).
- ¹⁵ D. W. McLaughlin and A. C. Scott, Phys. Rev. A **18**, 1652 (1978).
- ¹⁶ A. Barone, J. Appl. Phys. **42**, 2747 (1971).
- ¹⁷ A. C. Scott and W. J. Johnson, Appl. Phys. Lett. **14**, 316 (1969).
- ¹⁸ S. Pace and U. Gambardella, J. Low. Temp. Phys. **62**, 197 (1986).
- ¹⁹ A. V. Ustinov, H. Kohlstedt, and P. Henne, Phys. Rev. Lett. **77**, 3617 (1996).
- ²⁰ P. Cikmacs, M. Cirillo, V. Merlo, and R. Russo, IEEE Trans. Appl. Sup. **11**, 99 (2001).